# Synthesis and structural studies of polynuclear ruthenium clusters derived from reactions of 1,2,3,4-tetraphenyl-1,2,3,4-tetraphospholane with [Ru₃(CO)₁₂]

Xinhua Zhong *, Siau-Gek Ang, How-Ghee Ang

*Department of Chemistry, National University of Singapore, Singapore 119260, Singapore*

## Abstract

Reactions of 1,2,3,4-tetraphenyl-1,2,3,4-tetraphospholane (**I**) with triruthenium dodecacarbonyl at different temperatures result in the cleavage of P–P bonds and even P–C bond(s) in **I** to afford a series of new ruthenium cluster derivatives containing phosphido and phosphinidene ligands: a penta-ruthenium wing-tip bridged butterfly cluster $[Ru_5(CO)_{11}(\mu_4\text{-}PPh)(\mu_3\text{-}PPh)\{(\mu_4\text{-}\eta^2\text{-}(PPh)_2CH_2\}]$ (**1**), a hepta-ruthenium polyhedral (consisting of two fused square pyramids with a co-apex) cluster $[Ru_7(CO)_{15}(\mu_4\text{-}PPh)_2\{(\mu_2\text{-}PPh)_2CH_2\}]$(**2**), a linked penta-ruthenium cluster $[Ru_4(CO)_{10}(\mu_4\text{-}PPh)(\mu_3\text{-}PPh)_2(\mu_3\text{-}\eta^2\text{-}PPhCH_2)Ru(CO)_3]$ (**3**), and a hepta-nuclear polyhedral (consisting of two fused square pyramids with different apexes) cluster $[Ru_7(CO)_{15}(\mu_4\text{-}PPh)_2\{(\mu_2\text{-}PPh)_2CH_2\}]$(**4**). Clusters **2** and **4** are isomeric and differ only in the connection of the two square pyramids in the $Ru_7$ polyhedron. All the newly obtained clusters have been fully characterized by spectroscopic (IR, FABMS, ¹H- and ³¹P-NMR spectroscopy) and analytical techniques, and their molecular structures are established by single crystal X-ray diffraction analysis.
© 2003 Elsevier B.V. All rights reserved.

*Keywords:* Ruthenium cluster; Cyclopolyphosphine; Tetraphospholane; Crystal structure

## 1. Introduction

In recent years, there has been increasing interest in preparing phosphido-bridged and phosphinidene-capped tri- and polynuclear transition metal carbonyl cluster derivatives mainly due to their low tendency to fragment into monometallic species and consequently to their potential uses in many stoichiometric and catalytic reactions [1–3]. Such reported clusters containing edge-bridged and capped phosphine ligands have been synthesized mainly from the reactions of alkyl, aryl primary or secondary phosphines, cyclopolyphosphines, or carbon-chain polyphosphines with appropriate carbonyl clusters [4–8]. Cyclocarbophosphines containing P–P bond(s) can serve as potentially good phosphido and phosphinidene sources to stabilize polynuclear clusters

because of preferential P–P bond(s) rupture involved in the ring opening reactions under forced conditions [9].

Herein, we extend our studies on the reactions of $[(PPh)_4CH_2]$ (**I**) with triruthenium cluster $[Ru_3(CO)_{12}]$ [9a], whereupon several new polynuclear cluster derivatives with unusual structures are obtained. These include the rarely encountered $\mu_3$-coordination mode for one phosphido atom in $[Ru_5(CO)_{11}(\mu_4\text{-}PPh)(\mu_3\text{-}PPh)\{(\mu_4\text{-}\eta^2\text{-}(PPh)_2 CH_2\}]$ (**1**), and the first reported isomeric pair of heptaruthenium carbonyl clusters $[Ru_7(CO)_{15}(\mu_4\text{-}PPh)_2\{(\mu_2\text{-}PPh)_2CH_2\}]$ (**2**) and (**4**) consisting of two fused square pyramidal metal skeletons with or without a co-apex.

## 2. Results and discussion

### 2.1. Reactivity

Reactions of $[(PPh)_4CH_2]$ (**I**) with a twofold molar amount of $[Ru_3(CO)_{12}]$ at elevated temperatures in

---

* Corresponding author. Tel.: +65-68744569; fax: +65-68723564.
*E-mail address:* zhong_xinhua@alumni.nus.edu.sg (X. Zhong).

toluene result in the rupture of P–P and even P–C bonds in **I** to afford a series of penta- and hepta-nuclear ruthenium cluster derivatives containing phosphido and phosphinidene ligands which were separated by preparative thin-layer chromatography (TLC) (Scheme 1). From the reaction at 80 °C, $[Ru_5(CO)_{11}(\mu_4\text{-PPh})(\mu_3\text{-PPh})\{(\mu_4\text{-}\eta^2\text{-}(PPh)_2CH_2\}]$(**1**) and $[Ru_7(CO)_{15}(\mu_4\text{-PPh})_2\{(\mu_2\text{-PPh})_2CH_2\}]$(**2**) are obtained in 18% and 10% yields respectively. When the reaction is performed at 110 °C, one new compound can be isolated and identified as $[Ru_4(CO)_{10}(\mu_4\text{-PPh})(\mu_3\text{-PPh})_2(\mu_3\text{-}\eta^2\text{-PPhCH}_2)$ $Ru(CO)_3]$ (**3**) together with Cluster **2**, in 7% and 12% yields, respectively. Only $[Ru_7(CO)_{15}(\mu_4\text{-PPh})_2\{(\mu_2\text{-PPh})_2CH_2\}]$(**4**) in 13% yield can be obtained and characterized when the reaction is carried out at 140 °C. All the compounds were fully characterised by elementary analysis, IR, ^{1}H and ^{31}P NMR spectroscopy and their molecular structures were established by X-ray crystallography. The IR and NMR data of all the obtained clusters are collected in Table 1. The carbonyl stretching
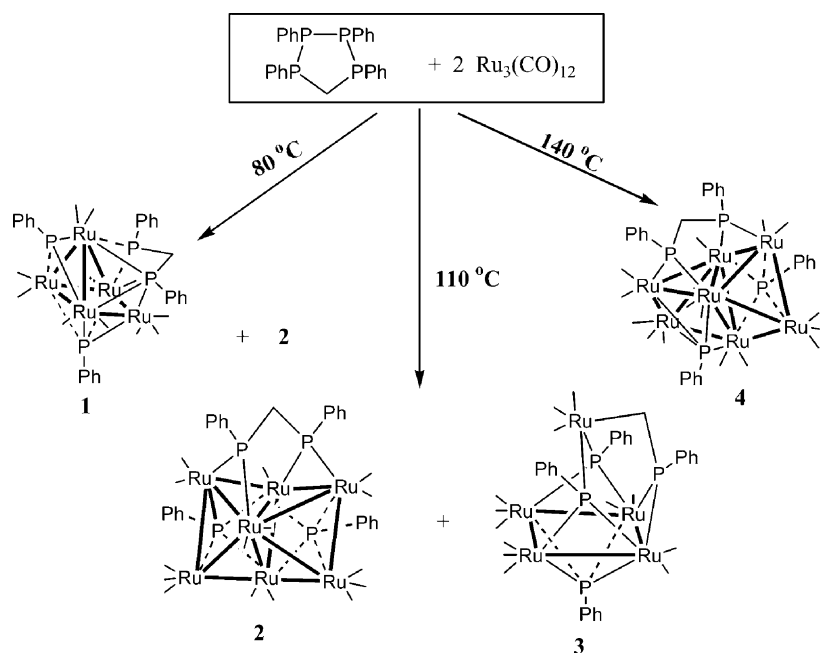


Scheme 1.

Table 1
Spectroscopic data for Clusters **1–4**

| | IR, $v$(CO) (cm$^{-1}$)[a] | ^{1}H-NMR, $\delta$ (J Hz)[b] | ^{31}P{^{1}H}-NMR, $\delta$ (J Hz)[b] | MS ($m/z$)[c] |
|---|---|---|---|---|
| **1** | 2061m, 2034s, 2023vs, 2008s, 1976w | 7.2–8.2(m, 20H, Ph) 5.45(m, 2H, CH$_2$) | 489.2 (dd, 98.2, 53.3, P$^1$ or P$^3$) 449.4(ddd, 87.4, 53.3, 10.6, P$^1$ or P$^3$) 127.7(ddd, 98.2, 87.4, 40.0, P$^2$) −40.8(dd, 40.0, 10.6, P$^4$) | 1260 (1260) |
| **2** | 2078m, 2053s, 2026s, 2009vs, 1983w | 7.3–8.0(m, 20H, Ph) 6.13(m, 1H, CH$_2$) 5.25(m, 1H, CH$_2$) | 484.8(m, P$^1$ or P$^2$) 484.1(m, P$^1$ or P$^2$) 225.8(dd, 50.7, 36.0, P$^3$ or P$^4$) 187.2(dd, 106.6, 50.7, P$^3$ or P$^4$) | 1574 (1574) |
| **3** | 2089m, 2071s, 2061s, 2049s, 2032vs, 2009s | 7.1–8.3(m, 20H, Ph) 4.20(m, 2H, CH$_2$) | 530.1(d, 42.7, P$^4$); 322.2(m, 42.7, 33.6, P$^2$) 171.8(d, 33.6, P$^1$ and P$^3$) | 1316 (1316) |
| **4** | 2074m, 2051vs, 2024s, 2019sh, 1954w | 7.2–8.0(m, 20H, Ph) 6.07(m, 1H, CH$_2$) 5.35(m, 1H, CH$_2$) | 525.4(dd, 28.0, 26.7, P$^1$ or P$^3$) 479.7(dd, 40.7, 28.0, P$^1$ or P$^3$) 243.9(dd, 49.6, 26.7, P$^2$ or P$^4$) 195.1(dd, 49.6, 40.7, P$^2$ or P$^4$) | 1574 (1574) |

[a] In CH$_2$Cl$_2$.
[b] In CDCl$_3$ with SiMe$_4$ for ^{1}H and 85% H$_3$PO$_4$ for ^{31}P as references.
[c] Simulated values are given in parentheses.

vibrations of all the clusters fall in the region between 1900 and 2200 $cm^{-1}$ indicating that all carbonyl groups on these clusters are terminal. The reaction products cannot be isolated and characterized when different molar ratios (1:1, or 2:1) of ligand to cluster are used. The excess of cluster in the reaction may favor the formation of polynuclear clusters which results from the further addition of $Ru(CO)_n$ into the precursor or intermediate lower nuclearity clusters. In the case of not excess of cluster in the reaction, lower nuclearity clusters may form. For the formed lower nuclearity clusters, maybe due to the low stability, or the low yield, we cannot isolate the formed products.

### 2.1.1. Cluster $[Ru_5(CO)_{11}(\mu_4-PPh)(\mu_3-PPh)\{(\mu_4-\eta^2-(PPh)_2CH_2\}](1)$

The molecular structure of Cluster **1** is illustrated in Fig. 1 together with the atomic labeling scheme and the relevant structure parameters are in Table 2. In the metal core of the cluster, five ruthenium atoms make up a pentagonal wing-tip bridged butterfly skeleton with Ru(2), Ru(1), Ru(5) and Ru(3) forming the butterfly and Ru(4) bridging the two wing-tip atoms of Ru(2) and Ru(3). The bridged-butterfly metal skeleton is capped by a $\mu_3$-PPh, a $\mu_4$-PPh and a bi-functional 6e-donor $\{\mu_4-\eta^2-(PPh)_2CH_2\}$ groups. The number of valence electrons for this cluster is 76, which is two more than the magic number for square pyramidal pentanuclear system [10], so one bonding orbital is converted into non-bonding to house the two excess electrons and the molecule has one metal-metal bond less than the square-based pyramid. The Ru–Ru bond distances vary over a wide range, from 2.8291(3) for Ru(1)–Ru(3) to 3.0390(3) Å for Ru(3)–Ru(5). The unbounded Ru(2) and Ru(3) atoms have a distance of 3.750(1) Å.

All P–P bonds in the $P_4C$-ring of the ligand **I** undergo breakage, leading to the $\mu_3$-PPh, $\mu_4$-PPh and $\{\mu_4-\eta^2-(PPh)_2CH_2\}$ fragments, which are captured by the cluster. The two phosphido atoms in the bifunctional group $\{\mu_4-\eta^2-(PPh)_2CH_2\}$ have different coordination environments. P(2) bridges over one wing edge of Ru(2)–Ru(5) with nearly equal distances, while P(4) caps a bent tri-nuclear chain of Ru(4)–Ru(3)–Ru(5) with different distances. The distance of P(4)–Ru(3) (2.8139(8) Å) is the longest one in all the P–Ru distances, but it still should be considered as a bond because it is shorter than the 2.864(2) Å in $[Ru_4(CO)_{14}(\mu-PCF_3)]$ [11] and shortly larger than the 2.779 Å in $[Ru_3(CO)_9(\mu-H)(\mu-PPh)]$ [12] and the 2.759 Å in $Ru_4(CO)_{13}(\mu-H)_2(\mu-PCF_3)]$ [13]. It is very unusual for a $PR_2$ phosphido group to adopt a $\mu_3$-coordination mode. Because of the unusual coordination mode in P(4), all the P–Ru distances associated with P(4) are exceptionally long with average value of 2.4160 (8) Å, which are significantly longer than all the other P–Ru distances in the cluster. The two phosphido atoms P(2) and P(4) atoms are separated by a distance of 2.6587(11) Å, which is significantly longer than the covalent radii (2.12 Å) for two P atoms, and thus cannot be considered as a bond. The known longest P–P bond length is 2.277 Å for $\{(2,4,6-Bu^tC_6H_2)P\}_2C=CCl_2$-cyclo in cyclopolyphosphine compounds [14].

Table 2
Selected bond lengths (Å) and angles (°) for Cluster **1**

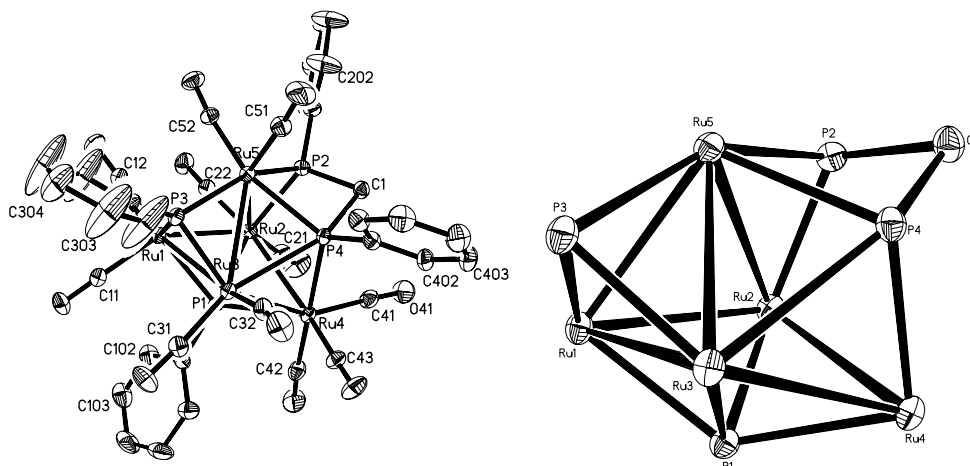| Bond Lengths | | | |
|---|---|---|---|
| Ru(1)–Ru(2) | 2.8498(3) | Ru(1)–Ru(3) | 2.8291(3) |
| Ru(1)–Ru(5) | 2.8753(3) | Ru(2)–Ru(4) | 2.9799(3) |
| Ru(2)–Ru(5) | 2.9917(3) | Ru(3)–Ru(4) | 2.9225(3) |
| Ru(3)–Ru(5) | 3.0390(3) | P(1)–Ru(1) | 2.3673(8) |
| P(1)–Ru(2) | 2.3454(8) | P(1)–Ru(3) | 2.3963(8) |
| P(1)–Ru(4) | 2.4082(8) | P(2)–Ru(2) | 2.2677(8) |
| P(2)–Ru(5) | 2.3547(8) | P(3)–Ru(1) | 2.2341(8) |
| P(3)–Ru(3) | 2.2453(8) | P(3)–Ru(5) | 2.3487(8) |
| P(4)–Ru(3) | 2.8139(8) | P(4)–Ru(4) | 2.3889(8) |
| P(4)–Ru(5) | 2.4611(8) | C(1)–P(2) | 1.817(3) |
| C(1)–P(4) | 1.874(3) | Ru(2)$\cdots$Ru(3) | 3.750(1) |
| *Bond angles* | | | |
| P(2)–C(1)–P(4) | 92.15(14) | | |



Fig. 1. Molecular structure of Cluster **1**. The overall structure with H-atom omitted (right). The $Ru_5P_4C$ framework (left).

The $^{31}P\{^1H\}$ NMR spectrum shows four groups of resonance signals with equal intensity (see Table 1). The high-field resonance signal at −40.8 ppm is assigned to P(4) atom without controversy, because P(4) atom bridges two Ru atoms of Ru(4) and Ru(5) without direct M–M interaction, which has a significant effect on the upfield shift of the phosphorus atom bridging across the metals [15]. It is reasonable to assign the resonance signal at 127.7 ppm to the other phosphorus atom P(2) of $\mu_4$-(PPh)$_2$CH$_2$ unit because of the relatively large coupling constant $^2J_{PCP}$ (40.0 Hz) between them. The two downfield signals at 489.2 and 449.4 ppm correspond to the two phosphinidene groups P(1) and P(3) atoms, but we cannot definitely assign these two signals.

### 2.1.2. Cluster [Ru$_7$(CO)$_{15}$($\mu_4$-PPh)$_2${($\mu_2$-PPh)$_2$CH$_2$}] (2)

The crystal structure of 2 is shown in Fig. 2 together with the important structural parameters listed in Table 3. In the metal core of the molecular structure, seven ruthenium atoms constitute two square pyramids with a co-vertex fused through a triangular face Ru(1), Ru(2) and Ru(7). This arrangement of metal atoms is relatively rare and is the first example in Ru$_7$ clusters. In three of the limited number of fully characterized heptaruthenium carbonyl clusters [16–23], [Ru$_7$(CO)$_{18}$($\mu_4$-PPh)$_2$] [23], [Ru$_7$(CO)$_{14}$($\mu_4$-PBu$^t$)$_2$ ($\mu_3$-PBu$^t$)$_2$] [20], and [Ru$_7$ (CO)$_{15}$($\mu_4$-PPh)$_2$ ($\eta^6$-C$_6$H$_5$Me)] [18], the structures determined exhibit a metal skeleton consisting of two square pyramidal units sharing a triangular face, none of which sharing a co-apex. The two square bases share an edge (Ru(1)–Ru(2)) and have a dihedral angle of 65.0°. Each of the two square bases is capped by a $\mu_4$-PPh group. P(3) in the bifunctional group ($\mu_2$-PPh)$_2$CH$_2$ bridges a basal–basal edge of Ru(2)–Ru(6), while the

other phosphorus atom P(4) bridges an apical–basal edge of Ru(3)–Ru(7). Cluster 2 has 100 valence electrons as expected for two square pyramids sharing a triangular face and is therefore an electron-precise species. The Ru–Ru distances cover a wide range from 2.7583(10) Å for Ru(2)–Ru(6) to 3.0598(10) Å for Ru(4)–Ru(7). The average basal–basal Ru–Ru distance (2.8383 Å) is significantly shorter than the average apical–apical distance (2.9297 Å). The P–Ru distances in this cluster fall within the normal range of P–Ru distances with the longest 2.389(2) Å for P(1)–Ru(3), and the shortest 2.245(2) Å for P(3)–Ru(6).

The $^{31}P\{^1H\}$ NMR spectrum shows three groups of resonance signals with integral intensity ratio of 2:1:1. The resonances of the two phosphinidene groups have almost the same chemical shifts of 484.8 and 484.1 ppm
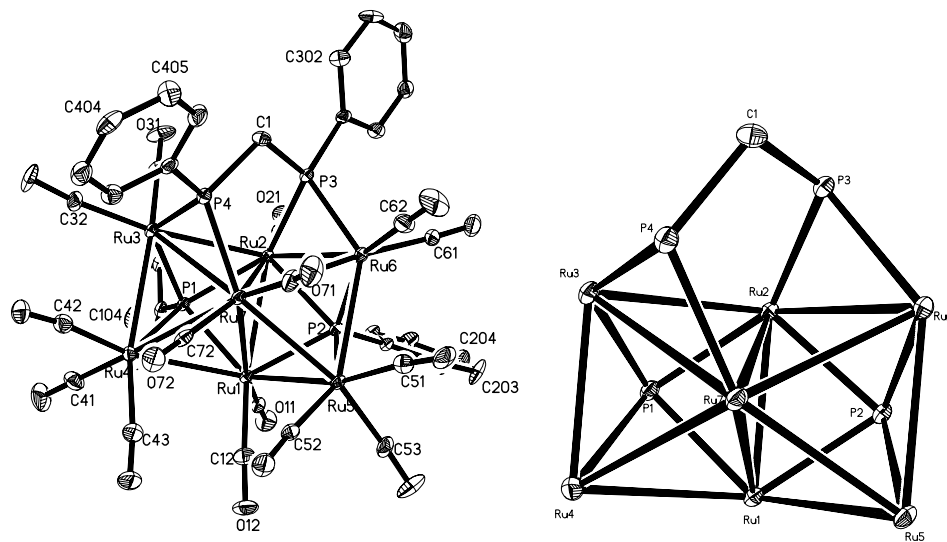
Table 3
Selected bond lengths (Å) and angles (°) for Cluster 2

| Bond lengths | | | |
|---|---|---|---|
| Ru(1)–Ru(2) | 2.8366(10) | Ru(2)–Ru(3) | 2.8742(10) |
| Ru(3)–Ru(4) | 2.8330(10) | Ru(4)–Ru(1) | 2.8276(10) |
| Ru(1)–Ru(5) | 2.8320(10) | Ru(5)–Ru(6) | 2.9066(10) |
| Ru(6)–Ru(2) | 2.7583(10) | Ru(7)–Ru(1) | 2.9164(10) |
| Ru(7)–Ru(2) | 2.8474(10) | Ru(7)–Ru(3) | 2.9200(10) |
| Ru(7)–Ru(4) | 3.0598(10) | Ru(7)–Ru(5) | 2.8675(10) |
| Ru(7)–Ru(6) | 2.9674(10) | P(1)–Ru(1) | 2.374(2) |
| P(1)–Ru(2) | 2.302(2) | P(1)–Ru(3) | 2.389(2) |
| P(1)–Ru(4) | 2.386(2) | P(2)–Ru(1) | 2.325(2) |
| P(2)–Ru(2) | 2.316(2) | P(2)–Ru(5) | 2.385(2) |
| P(2)–Ru(6) | 2.367(2) | P(3)–Ru(2) | 2.289(2) |
| P(3)–Ru(6) | 2.245(2) | P(4)–Ru(3) | 2.280(2) |
| P(4)–Ru(7) | 2.326(2) | P(3)–C(1) | 1.821(9) |
| P(4)–C(1) | 1.809(9) | | |
| | | | |
| Bond angles | | | |
| P(3)–C(1)–P(4) | 105.3(4) | | |



Fig. 2. Molecular structure of Cluster 2. The overall structure with H-atom and the solvent molecule (dichloromethane) omitted (right). The Ru$_7$P$_4$C framework (left).
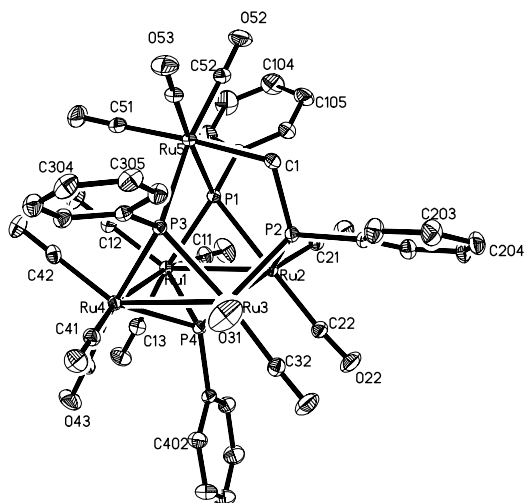
Fig. 3. Molecular structure of Cluster **3**. Hydrogen atoms and the solvent molecule (diethyl ether) are omitted for clarity.

Table 4
Selected bond lengths (Å) and angles (°) for Cluster **3**

| *Bond lengths* | | | |
|---|---|---|---|
| Ru(1)–Ru(2) | 2.9759(4) | Ru(2)–Ru(3) | 2.9210(4) |
| Ru(3)–Ru(4) | 2.9797(4) | Ru(4)–Ru(1) | 3.0232(4) |
| P(1)–Ru(1) | 2.4389(10) | P(1)–Ru(2) | 2.3742(9) |
| P(1)–Ru(5) | 2.4051(10) | P(2)–Ru(2) | 2.2906(10) |
| P(2)–Ru(3) | 2.2939(10) | P(3)–Ru(3) | 2.3761(9) |
| P(3)–Ru(4) | 2.4370(9) | P(3)–Ru(5) | 2.4079(10) |
| P(4)–Ru(1) | 2.3916(10) | P(4)–Ru(2) | 2.3594(9) |
| P(4)–Ru(3) | 2.3792(9) | P(4)–Ru(4) | 2.3706(9) |
| C(1)–P(2) | 1.833(4) | C(1)–Ru(5) | 2.191(4) |
| *Bond angles* | | | |
| P(2)–C(1)–Ru(5) | 114.62(18) | P(1)–Ru(5)–P(3) | 83.14(3) |

respectively which overlap severely. The two high-field shifts at 225.8 and 187.2 ppm correspond to the bifunctional phosphido group $(\mu_2\text{-PPh})_2CH_2$.

### 2.1.3. Cluster $[Ru_4(CO)_{10}(\mu_4\text{-Ph})(\mu_3\text{-PPh})_2(\mu_3\text{-}\eta^2\text{-}PPhCH_2)Ru(CO)_3]$ (**3**)

The molecular structure of cluster **3** together with the atomic numbering scheme is illustrated in Fig. 3. Selected bond lengths and angles are listed in Table 4. Four ruthenium atoms constitute a square plane which is linked to an isolated mononuclear $Ru(CO)_3$ unit through two $\mu_3$-PPh and a $\mu_3\text{-}\eta^2$-PPhCH$_2$ groups. A $\mu_4$-phenylphosphinidene group caps the square plane from below. The P–Ru distances cover a range from 2.2906(9) Å for P(2)–Ru(2) to 2.4389(10) Å for P(1)–Ru(1). Not only all the P–P bonds but also one P–C bond in the $P_4C$-ring of the ligand **I** are cleaved during the reaction process and thus results in three PPh and a PPhCH$_2$ fragments, which are captured by the cluster unit. The cleavage of the P–C bond in cyclocarbophosphine system is not usually encountered.

The $^{31}P\{^1H\}$ NMR spectrum exhibits three groups of peaks (see Table 1). Because the two tridentate coordinated phosphinidene groups P(1) and P(3) are chemically equivalent, the signal at 171.8 ppm is assigned to those two P atoms. The unusual high-field shifts of P(1) and P(3) may be partly due to their bonding metal atoms not directly interacting to each other [15]. It is reasonable to assign the low-field shift at 530.1 ppm to the $\mu_4$-phosphinidene P(4) atom and the remaining signal at 322.2 ppm to the phosphido P(2) atom.

### 2.1.4. Cluster $[Ru_7(CO)_{15}(\mu_4\text{-PPh})_2\{(\mu_2\text{-PPh})_2CH2\}]$ (**4**)

The X-ray structure of Cluster **4** is presented in Fig. 4 and the selected bond parameters are collected in Table 5. Clusters **4** and **2** are structurally isomeric differing in the arrangement of metal skeletons. Like the case of Cluster **2**, seven ruthenium atoms make up two square pyramids sharing a triangular face in **4**. Unlike Cluster **2**, the two fused square pyramids in **4** have different

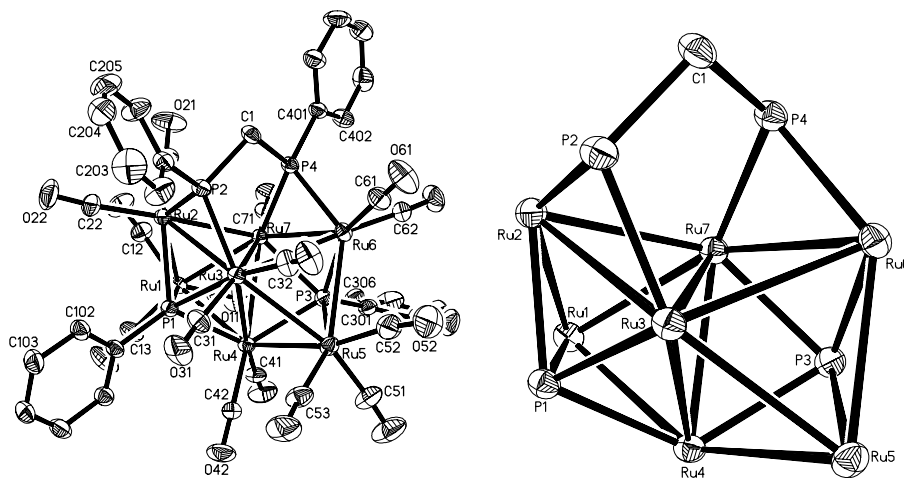

Fig. 4. Molecular structure of Cluster **4**. The overall structure with H-atom and the solvent molecule (dichloromethane) omitted (right). The Ru$_7$P$_4$C framework (left).

Table 5
Selected bond lengths (Å) and angles (°) for Cluster **4**

| Bond lengths | | | |
|---|---|---|---|
| Ru(1)–Ru(2) | 2.8646(7) | Ru(2)–Ru(3) | 2.9124(7) |
| Ru(3)–Ru(4) | 2.9049(7) | Ru(4)–Ru(1) | 2.8688(7) |
| Ru(4)–Ru(5) | 2.8051(7) | Ru(5)–Ru(6) | 2.9089(7) |
| Ru(6)–Ru(7) | 2.7485(7) | Ru(7)–Ru(4) | 2.8639(6) |
| Ru(3)–Ru(5) | 2.9212(7) | Ru(3)–Ru(6) | 3.0144(7) |
| Ru(3)–Ru(7) | 2.8480(6) | Ru(7)–Ru(1) | 2.8228(7) |
| Ru(7)–Ru(2) | 2.7400(7) | P(1)–Ru(1) | 2.348(2) |
| P(1)–Ru(2) | 2.358(2) | P(1)–Ru(3) | 2.476(2) |
| P(1)–Ru(4) | 2.308(2) | P(2)–Ru(2) | 2.228(2) |
| P(2)–Ru(3) | 2.326(2) | P(3)–Ru(4) | 2.345(2) |
| P(3)–Ru(5) | 2.387(2) | P(3)–Ru(6) | 2.378(2) |
| P(3)–Ru(7) | 2.312(2) | P(4)–Ru(6) | 2.280(2) |
| P(4)–Ru(7) | 2.279(2) | P(2)–C(5) | 1.828(6) |
| P(4)–C(5) | 1.829(6) | | |
| | | | |
| Bond angles | | | |
| P(2)–C(5)–P(4) | 103.9(3) | | |

apexes. The Ru–Ru bond distances cover a wide range, from 2.7402(6) Å for Ru(2)–Ru(7) to 3.0148(6) Å for Ru(3)–Ru(6) with the average basal–basal Ru–Ru distance (2.8596 Å) a little shorter than the average apical–basal distance (2.8736 Å) which accords with the observation in Cluster **2**. The P–Ru distances associated with $\mu_2$-phosphido phosphorus atoms P(2) and P(4) (average value 2.278 Å) are significantly shorter than those from $\mu_4$-phosphinidene phosphorus atoms P(1) and P(3) (average value 2.364 Å).

The $^{31}P\{^1H\}$ NMR spectrum shows four groups of signals corresponding to four chemically different phosphorus atoms. The low-field chemical shifts at 525.4 and 479.7 ppm correspond to the two phosphinidene phosphorus atoms P(1) and P(3), while the high-field chemical shifts at 243.9 and 195.1 ppm correspond to the two phosphido phosphorus atoms P(2) and P(4).

## 3. Conclusion

The reactions of 1,2,3,4-tetraphenyl-1,2,3,4-tetraphospholane with $[Ru_3(CO)_{12}]$ occur with cleavage of all three P–P bonds but with retention of P–C bonds to form a series of ($\mu$-PPh)$_2$CH$_2$ bridged and phosphinidene-capped polynuclear Clusters **1**, **2** and **4**, or with rupture of one P–C bond to produce a ($\mu_3$-$\eta^2$-PPhCH$_2$) bridged Cluster **3**. The M–M bonds in ruthenium clusters can be easily broken and rearrange to form polynuclear clusters stabilized by phosphinidene and phosphido ligands. The $^{31}P$ shift for phosphinidene groups in these obtained clusters show low-field shifts at around 500 ppm. The $^{31}P$ shift for the phosphido bridging non-metal–metal bond is shifted upfield compared with that for the phosphido bridging metal–metal bond.

## 4. Experimental

### 4.1. General

All reactions described above were carried out in vacuo (around 10 mbar) using reaction vessels equipped with Teflon taps. Analytical grade solvents were distilled prior to use under nitrogen atmosphere over appropriate drying agents. Products were separated by preparative TLC using laboratory-prepared $20 \times 20$ cm glass plates coated to thickness of 0.3 mm with Merck Kieselgel $60F_{254}$ silica gel. Mixture of dichloromethane and hexane was used in various proportions as eluents for TLC. The starting materials $[Ru_3(CO)_{12}]$ and $[(PPh)_4CH_2]$ were prepared by literature methods [24,25]. Elemental analysis was carried out at the Microanalytical Laboratory, National University of Singapore. Infrared spectra were recorded as solution in 0.5 mm KBr cell on a Bio-Rad FTS-165 spectrometer, $^1H$ and $^{31}P$ NMR spectra on Bruker 500 MHz Fourier-Transform spectrometers using SiMe$_4$ (for $^1H$) and 85% H$_3$PO$_4$ solution (for $^{31}P$) as references and mass spectra on a Finnigan MAT 95 instrument by the fast atom bombardment technique, using $\alpha$-nitrobenzyl alcohol or thioglycerol as the matrix solvent.

All single crystals for X-ray diffraction analysis were obtained by slow evaporation of a saturated CH$_2$Cl$_2$–hexane solution or by slow diffusion of ether into a saturated dichloromethane solution in −20 °C refrigerator for several days. Crystal data and details of the measurement for clusters **1**–**4** are given in Table 6. Diffraction intensities were collected at 293 K on a Siemens CCD SMART system. The structures were solved by direct methods and refinement was by the full-matrix, least-squares method with all non-hydrogen atoms refined anisotropically. All calculations were carried out using a SHELXTL software package [26].

### 4.2. Reactions of $[Ru_3(CO)_{12}]$ with $[(PPh)_4CH_2]$ (I)

#### 4.2.1. At 80 °C

The compound $[Ru_3(CO)_{12}]$ (200 mg, 0.31 mmol) and **I** (71 mg, 0.16 mmol) were placed in one tube of a double reaction vessel, and degassed under vacuo. Freshly distilled toluene (10 cm$^3$) was placed in the other tube of the reaction vessel. After degassing with three freeze–pump–thaw cycles, the solvent was then transferred to the other tube containing the reactants. The reaction mixture was heated with stirring at 80 °C oil bath for 18 h. The color of the reaction mixture turned red then dark red in half hour. The resultant dark red solution was evaporated to dryness under reduced pressure. The residue was dissolved in the minimum volume of CH$_2$Cl$_2$ and separated by TLC using CH$_2$Cl$_2$–hexane (1:4 v/v) as eluent. Two major bands of dark red Cluster **1** ($R_f$ = 0.47, 43 mg, 18%) and Cluster **2** ($R_f$ = 0.38, 21 mg, 10%) were eluted

Table 6
Summary of crystal data and data collection parameters for Clusters **1–4**

| Compound | **1** | **2** | **3** | **4** |
|---|---|---|---|---|
| Formula | $C_{36}H_{22}O_{11}P_4Ru_5$ | $C_{40}H_{22}O_{15}P_4Ru_7 \cdot CH_2Cl_2$ | $C_{38}H_{22}O_{13}P_4Ru_5 \cdot 1/2(C_2H_5)_2O$ | $C_{40}H_{22}O_{15}P_4Ru_7 \cdot 2CH_2Cl_2$ |
| Formula weight | 1259.77 | 1658.87 | 1352.85 | 1708.35 |
| Crystal system | Monoclinic | Triclinic | Monoclinic | Monoclinic |
| Space group | $P2(1)/n$ | $P\bar{1}$ | $P2_1/n$ | $C2/c$ |
| $a$ (Å) | 10.1683(1) | 11.5094(2) | 11.1128(1) | 42.8424(3) |
| $b$ (Å) | 19.4500(2) | 16.9630(3) | 21.5245(3) | 12.2548(2) |
| $c$ (Å) | 21.0377(1) | 14.9840(3) | 20.1196(2) | 22.8682(2) |
| $\alpha$ (°) | | 98.362(1) | | |
| $\beta$ (°) | 97.971(1) | 95.289(1) | 97.377(1) | 116.12(1) |
| $\gamma$ (°) | | 96.782(1) | | |
| $V$ (Å$^3$) | 4120.50(6) | 2519.42(8) | 4772.72(9) | 10779.8(2) |
| $Z$ | 4 | 2 | 4 | 8 |
| $\mu$ (mm$^{-1}$) | 2.002 | 2.338 | 1.740 | 2.237 |
| Reflections measured | 26235 | 23827 | 43807 | 34445 |
| Unique reflections | 10239 | 12268 | 12101 | 13430 |
| $R_{int}$ | 0.0269 | 0.0544 | 0.0331 | 0.0550 |
| $[I > 2\sigma(I)]$ | $R_1 = 0.0284$, $wR_2 = 0.0582$ | $R_1 = 0.0543$, $wR_2 = 0.1212$ | $R_1 = 0.0291$, $wR_2 = 0.0830$ | $R_1 = 0.0439$, $wR_2 = 0.0879$ |
| All data | $R_1 = 0.0402$, $wR_2 = 0.0633$ | $R_1 = 0.1051$, $wR_2 = 0.1411$ | $R_1 = 0.467$, $wR_2 = 0.0900$ | $R_1 = 0.0895$, $wR_2 = 0.1052$ |
| $S(F^2)$ | 1.032 | 0.948 | 1.077 | 0.986 |
| Temperature (K) | 293(2) | 293(2) | 293(2) | 293(2) |

and collected (Found for **1**: C, 34.56; H, 1.86; P, 9.03; Calc. for $C_{36}H_{22}O_{11}P_4Ru_5$: C, 34.32; H, 1.76; P, 9.83. Found for **2**: C, 30.93; H, 1.57; P, 7.23; Calc. for $C_{40}H_{22}O_{15}P_4Ru_7$: C, 30.52; H, 1.41; P, 7.87).

### 4.2.2. At 110 °C

Reaction conditions were similar to those described in Section 4.2.1. TLC afforded six major bands, but only red Cluster **3** from band 1 ($R_f = 0.59$, 18 mg, 7%) and dark red Cluster **2** from band 4 ($R_f = 0.36$, 25 mg, 12%) were characterized. (Found for **3**: C, 34.34; H, 1.82; P, 8.93; Calc. for $C_{38}H_{22}O_{13}P_4Ru_5$: C, 34.69; H, 1.69 ; P, 9.42).

### 4.2.3. At 140 °C

The reaction conditions were similar to those described in Section 4.2.1. TLC afforded two major bands, but only dark red Cluster **4** from band 2 were characterized ($R_f = 0.40$, 35 mg, 13%) (Found for **4**: C, 30.89; H, 1.64; P, 7.34; Calc. for $C_{40}H_{22}O_{15}P_4Ru_7$: C, 30.52; H, 1.41; P, 7.87).

## 5. Supplementary material

Crystallographic data for the structural analysis have been deposited with the Cambridge Crystallographic Data Center, CCDC nos. 207702, 183939, 207703, 183941 for compounds **1–4**, respectively.

## Acknowledgements

## References

[1] P.Y. Zheng, T.T. Nadasdi, D.W. Meek, Organometallics 8 (1989) 1393.

[2] P.E. Fuchs, M.R. Gregg, J. Phillips, M.V.R. Stainer, Organometallics 9 (1990) 387, and references cited therein.

[3] G.G. Hlatky, R.H. Crabtree, Coord. Chem. Rev. 65 (1985) 1;
M.A. Ansari, J.A. Ibers, Coord. Chem. Rev. 100 (1990) 223;
L.C. Roof, J.W. Kolis, Chem. Rev. 93 (1993) 1037;
F. Basolo, Coord. Chem. Rev. 125 (1993) 13.

[4] F. Iwasaki, M.J. Mays, P.R. Raithby, P.L. Taylor, P.J. Wheatley, J. Organomet. Chem. 213 (1981) 185;
K. Natarajan, O. Scheidsteger, G. Huttner, J. Organomet. Chem. 221 (1981) 301.

[5] J.S. Field, R.J. Haines, D.N. Smit, J. Chem., Soc. Dalton Trans. (1988) 1315.

[6] A.J. Deeming, S.D. Mtunzi, S.E. Kabir, J. Organomet. Chem. 276 (1984) C65.

[7] B.F.G. Johnson, T.M. Layer, J. Lewis, P.R. Raithby, W.T. Wong, J. Chem. Soc., Dalton Trans. (1993) 973.

[8] L.M. Bullock, J.S. Field, R.J. Haines, E. Minshall, M.H. Moore, F. Mulla, D.M. Smit, L.M. Steer, J. Organomet. Chem. 381 (1990) 429.

[9] (a) S.G. Ang, X. Zhong, H.G. Ang, J. Chem. Soc., Dalton Trans. (2001) 1151;
(b) S.G. Ang, X. Zhong, H.G. Ang, Inorg. Chem. 41 (2002) 3791;
(c) S.G. Ang, X. Zhong, H.G. Ang, Phosphorous, Sulfur Silicon 177 (2002) 1463;
(d) S.G. Ang, X. Zhong, H.G. Ang, J. Organomet. Chem. 665 (2003) 218.

[10] D.M.P. Mingos, J. Chem. Soc., Commun. (1983) 706.

[11] H.G. Ang, K.W. Ang, S.G. Ang, A.L. Rheingold, J. Chem. Soc., Dalton Trans. (1996) 3131.

[12] S.A. MacLaughlin, A.J. Carty, N.J. Taylor, Can. J. Chem. 60 (1982) 87.

[13] H.G. Ang, S.G. Ang, S. Du, B.H. Sow, X. Wu, J. Chem. Soc., Dalton Trans. (1999) 2799.

[14] M. Gougou, C. Tachon, R. Elouatib, O. Ramarijaona, G. Etemadmoghadam, M. Koenig, Tetrahed. Lett. 30 (1989) 177.

[15] A.J. Carty, S.A. MacLaughlin, D. Nucciarone, in: J.G. Verkade, L.D. Quinn (Eds.), Phosphorus-31 NMR Spectroscopy in Stereochemical Analysis: Stereochemistry of Metal Complexes: Phosphido Bridging Ligands, VCH publishers, New York, 1987 (Chapter 16).

[16] B.F.G. Johnson, D.S. Shephard, D. Braga, F. Grepioni, S. Parsons, J. Chem. Soc., Dalton Trans. (1998) 311.

[17] J. Lewis, C.A. Morewood, P.R. Raithby, C.R. Arellano, J. Chem. Soc., Dalton Trans. (1997) 3335.

[18] E. Charalambous, L. Heuer, B.F.G. Johnson, J. Lewis, W.-S. Li, M. McPartlin, A.D. Massey, J. Organomet. Chem. 468 (1994) C9.

[19] C.E. Housecroft, A.L. Rheingold, X. Song, Inorg. Chem. 31 (1992) 4023.

[20] K.J. Edwards, J.S. Field, R.J. Haines, F.J. Mulla, J. Organomet. Chem. 402 (1991) 113.

[21] P. Frediani, M. Bianchi, A. Salvani, F. Piancenti, S. Ianelli, M. Nardelli, J. Chem. Soc., Dalton Trans. (1990) 1705.

[22] (a) R.D. Adams, J.T. Babin, M. Tanner, Organometallics 7 (1998) 503;
(b) R.D. Adams, J.T. Babin, M. Tasi, Organometallics 7 (1998) 2027.

[23] F.V. Gastel, N.J. Taylor, A.J. Carty, J. Chem. Soc., Chem. Commun. (1987) 1049.

[24] M.I. Bruce, C.M. Jensen, N.L. Jones, Inorg. Synth. 26 (1989) 259.

[25] M. Baudler, J. Vesper, P. Junkes, H. Sandmann, Angew. Chem. Int. Ed. 10 (1971) 940.

[26] SHELXTL, version 5.1, Brucker AXS, Inc., Madison, WI, 1997.